

1 Drought **conditions** disrupt atmospheric carbon uptake 2 in a Mediterranean saline lake

3 Ihab Alfadhel^{1,2}, Ignacio Peralta-Maraver^{1,2,3*}, Isabel Reche^{1,2,3}, Enrique P.
4 Sánchez-Cañete^{2,4,5}, Sergio Aranda-Barranco^{1,4}, Eva Rodríguez-Velasco^{1,2,3},
5 Andrew S. Kowalski^{2,4,5}, Penélope Serrano-Ortiz^{1,4*}.

6 7 *Authors adress:*

8 ¹Departamento de Ecología, Facultad de Ciencias, Universidad de Granada, Granada,
9 Spain.

10 ²Instituto del Agua, Granada, Universidad de Granada, Spain.

11 ³Research Unit Modeling Nature (MNat), Universidad de Granada, Granada, Spain.

12 ⁴Instituto Interuniversitario de Investigación del Sistema Tierra en Andalucía (IISTA),
13 Universidad de Granada, Spain

14 ⁵Departamento de Física Aplicada, Universidad de Granada, Granada, Spain.

15
16 **Correspondence to:* Ignacio Peralta-Maraver (peraltamaraver@ugr.es) and Penélope
17 Serrano-Ortiz (penelope@go.ugr.es).

18
19 **Abstract:** Saline inland lakes play a key role in the global carbon cycle, acting as
20 dynamic zones for atmospheric carbon exchange and storage. Given the global decline of
21 saline lakes and the expected increase of periods of drought in a climate change scenario,
22 changes in their potential capacity to uptake or emit atmospheric carbon are expected.
23 Here, we conducted continuous measurements of CO₂ and CH₄ fluxes at the ecosystem
24 scale in a saline endorheic lake of the Mediterranean region over nearly 2 years. Our focus
25 was on determining net CO₂ and CH₄ exchanges with the atmosphere under both dry and
26 flooded conditions, using the eddy covariance (EC) method. We coupled greenhouse gas
27 flux measurements with water storage and analyzed meteorological variables like air
28 temperature and radiation, known to influence carbon fluxes in lakes. This extensive data
29 integration enabled the projection of the net carbon flux over time, accounting for both
30 dry and wet conditions on an interannual scale. **We found that the system acts as a**
31 **substantial carbon sink by absorbing atmospheric CO₂ under wet conditions. In years with**
32 **prolonged water storage, it is predicted that the lake's CO₂ assimilation capacity can**

33 surpass -0.7 kg C m^2 annually. Conversely, during extended drought years, a reduction in
34 CO_2 uptake capacity of more than 80% is expected. Regarding CH_4 , we measured uptake
35 rates that exceeded those of well-aerated soils such as forest soils or grasslands, reaching
36 values of $-0.2 \mu\text{mol m}^{-2} \text{ s}^{-1}$. Additionally, we observed that CH_4 uptake during dry
37 conditions was nearly double that of wet conditions. However, the absence of continuous
38 data prevented us from correlating CH_4 uptake processes with potential environmental
39 predictors. Our study challenges the widespread notion that wetlands are universally
40 greenhouse gas emitters, highlighting the significant role that endorheic saline lakes can
41 play as natural sink of atmospheric carbon. However, our work also underscores the
42 vulnerability of these ecosystem services in the current climate change scenario, where
43 drought episodes are expected to become more frequent and intense in the coming years.

44

45 **Keywords:** Intermittent saline lake, eddy covariance, greenhouse gas fluxes, ecosystem
46 metabolism, Mediterranean shallow lake

47

48 1. Introduction

49 Saline inland lakes are diverse and play a crucial role in the global carbon cycle, serving
50 as dynamic zones for carbon dioxide exchange with the atmosphere (Li et al. 2022; Liao
51 et al. 2024) and long-term sinks of organic and inorganic carbon (Anderson and Stedmon
52 2007; Song et al. 2013; Li et al. 2017). In limnology, however, the ecological importance
53 of these systems has only recently been recognized, despite accounting for approximately
54 44% of global lake volume and 23% of lake surface area (Messenger et al., 2016). Saline
55 lakes vary in size from ephemeral ponds to extensive deep-water bodies, such as the
56 Caspian Sea (Eugster and Hardie, 1978). These lakes are characterized by salinity levels
57 that exceed 3 parts per thousand and are notably isolated from a direct marine influence
58 (Williams, 2002; Wang et al., 2018). They are found in endorheic (hydrologically
59 landlocked) basins across a wide array of climates, spanning cold to warm/hot arid
60 regions in all continents, including Antarctica (Williams, 2002; Wang et al., 2018). As
61 terminal points in many hydrological networks, they collect not only significant amounts
62 of salts but also nutrients and organic and inorganic carbon (Anderson and Stedmon 2007;
63 Song et al. 2013; Batanero et al. 2017; Li et al. 2017; Liao et al. 2024).

64 Past estimations about the role of saline lakes on global carbon fluxes suggested
65 that these lakes might function as hotspots for the CO_2 emission (Duarte et al., 2008).

66 However, more recent works point out that saline lakes have lower partial pressure of
67 CO₂ than freshwater lakes (Wen et al. 2017) and some systems appear to take up CO₂
68 during the winter (Li et al., 2022) or even annually (Yang et al. 2021) due to
69 physicochemical reactions and increased activity of primary producers. Therefore, more
70 seasonal studies on CO₂ fluxes in saline lakes are needed to understand the conditions
71 when these systems behave as sinks or sources of CO₂. Variations in CO₂ and CH₄ flux
72 estimates across different studies of water bodies are primarily due to the highly variable
73 data obtained from discrete sampling (Li et al. 2022) or because of differences in sampling
74 seasons at the intra-annual scale (Liao et al. 2024). Meanwhile, gathering continuous time
75 series data on CO₂ and CH₄ sequestration and emission fluxes over years is needed for
76 accurate assessment of the net carbon balance in inland water systems (Martínez-García
77 et al. 2024). Nevertheless, long-term, uninterrupted, and direct monitoring of greenhouse
78 gas flux dynamics at the ecosystem level is relatively scarce in aquatic ecosystems, and
79 this is particularly true for saline lakes. To the best of our knowledge, only a couple of
80 studies have reported continuous year-round direct measurements at the ecosystem scale
81 for CO₂ fluxes (Yang et al. 2021; Li et al. 2022). However, saline lakes' characteristics
82 differ with latitude (Hammer 1986) and could have very different behaviors regarding
83 carbon exchanges depending on climate conditions.

84 The carbon hydrochemistry in permanent saline lakes, especially in mountainous
85 and Arctic latitudes such as the Tibetan Plateau or Svalbard is largely influenced by
86 surface ice formation (Anderson et al., 2004; Rysgaard et al., 2012, 2013; Wu et al., 2014;
87 Yan and Zheng, 2015). In contrast, saline lakes in arid and semi-arid endorheic basins,
88 including Mediterranean climates, are typically shallow, often ephemeral, and/or
89 hypersaline due to evaporation exceeding precipitation (García et al., 1997; Batanero et
90 al. 2017; Saccò et al., 2021). The lower depths and higher surface-to-volume ratio, driven
91 by drought conditions, induce significant physicochemical fluctuations in these saline
92 inland water bodies, spanning from diurnal to interannual scales (Comin et al. 1990;
93 García and Niell 1991; García et al. 1997; Batanero et al. 2017). Consequently, the
94 precipitation regime and subsequent changes in groundwater levels determine the ecology
95 of saline lakes in arid and semi-arid regions. However, research on the interannual
96 variability of carbon fluxes in saline lakes affected by seasonal flooding and drought is
97 lacking. This knowledge gap urgently requires focused research to elucidate the impacts
98 of climatic variability on the carbon dynamics of these ecosystems, which have been
99 identified as particularly vulnerable to climate fluctuations (Tweed et al., 2011).

100 Furthermore, recent studies highlight a global decline in lake water storage in most
101 endorheic basins and in the Sahara, Arabia, and Southern Europe basin in particular
102 (Wang et al. 2018), a situation expected to worsen with more severe droughts in a climate
103 change scenario, leading to lower water levels and prolonged desiccation periods
104 (Wurtsbaugh et al., 2017; Hassani et al., 2020).

105 In this study, we carried out continuous and interannual measurements of CO₂ and
106 CH₄ fluxes at the ecosystem level in Spain's saline lake Fuente de Piedra using the Eddy
107 Covariance (EC) method. Serving as a model of a Mediterranean shallow saline lake, it
108 is characterized by sporadic episodes of water retention but predominantly dry during the
109 summer. It is worth noting that Fuente de Piedra Lake was designated as a Ramsar site in
110 1983, ensuring a rich history of monitoring water storage and the various meteorological
111 drivers of CO₂ and CH₄ fluxes. The objectives of our work are a) to quantify carbon
112 exchanges during the dry and the flooded conditions, determining its role as a carbon
113 source or sink, b) to evaluate main drivers promoting carbon exchange behaviors, and
114 finally c) Using available records of the time series for the main drivers of fluxes to model
115 the annual net carbon flux of the system in the past. Our research aims to enhance our
116 understanding of the carbon dynamics and the impacts of climate change on the net carbon
117 balance in Mediterranean intermittent endorheic lakes.

118

119 2. Material and methods

120 *Study Site*

121 Fuente de Piedra is a shallow and saline lake located in an endorheic basin in the province
122 of Málaga, Andalusia, Spain (37.11 N, -4.77 W, elevation 410 m: **Fig 1**). It spans
123 approximately 17 km², measuring 6.8 km in length and 2.5 km in width, with a maximum
124 depth of 1.5 meters. We take advantage of Fuente de Piedra Lake's inclusion in the
125 Ramsar Convention in 1983. This designation ensures a rich history monitoring of water
126 storage and the meteorological drivers discussed in this article. Such a comprehensive
127 dataset allows for the back projection of the net carbon flux of the system over time,
128 incorporating both dry and wet conditions at an interannual scale. This lake is recognized
129 as a vital habitat within a protected wetland at various levels—regional (as a natural
130 reserve), European (designated as a special bird protection area), and international
131 (acknowledged as a Ramsar site)—and offers an exemplary nesting ground for the pink
132 flamingo (*Phoenicopterus roseus*), largely due to its shallow waters. Among primary

133 producers, diatoms constitute the largest fraction of primary producers of the
134 **phytoplankton** all through the year, being dominated by *Hantzschia amphioxys*, *Amphora*
135 *coffeaiiformis*, *Stauronensis amphioxys*, *Cocconeis placentula*, *Entomoneis* sp. and
136 several species of *Navicula* and *Nitzschia* sp. (García and Niell, 1993).

137 Salinity levels in the lake vary significantly, ranging from oligosaline (5 ppt) to
138 hypersaline conditions (> 200 ppt), influenced by the annual hydrological cycle (Batanero
139 et al. 2017). **This cycle is delineated into two distinct phases: a pooling phase during**
140 **autumn and winter (December to March), and an evaporative and drought phase spanning**
141 **spring and summer (April to November).** The lake primarily receives water from
142 groundwater inflow (Rodríguez- Rodríguez et al. 2006), complemented by contributions
143 from two streams (**Fig. 1**) and surface runoff from surrounding farmlands. Notably, the
144 stream entering from the northeast adds nutrients. However, sediment samples distributed
145 across the lake and analyzed through combustion (Heiri et al., 2001) showed it to be
146 homogeneous in organic carbon (0.21 ± 0.07 mg C), nitrogen (0.015 ± 0.004 mg N) and the
147 C:N ratio (14.4 ± 2.3).

148

149 ***Field measurements of greenhouse gas fluxes and meteorological drivers.***

150 We employed the eddy covariance method to quantify the exchanges of CO₂, CH₄, and
151 energy (sensible and latent heat) every 30 min from August 2021 to May 2023. Thus, **the**
152 eddy covariance system was operated for more than 21 months, including two dry periods
153 in summer. An open-path eddy covariance (EC) system was strategically positioned atop
154 a tower, 3.1 meters above ground level, on the western bank of the lake (**Fig.1**). This setup
155 included two open-path infrared gas analyzers: the LI7500 for CO₂ and water vapor, and
156 the LI7700 for CH₄ (LICOR Inc., Lincoln, NE, USA). Wind vector components (u, v, w)
157 and sonic temperature were accurately measured using a sonic anemometer (R.M. Young
158 81000V, Traverse City, MI, USA). **These data were recorded on a data logger (CR1000,**
159 **Campbell Scientific, Logan, UT, USA) at a frequency of 10Hz.**

160 In addition to gas measurements, we measured a comprehensive suite of
161 environmental and soil state variables every 10 seconds to capture the conditions over a
162 representative ground surface area and collected every 30 min average by a data logger
163 (CR1000, Campbell Scientific, Logan, UT, USA). Air temperature (T_a) and relative
164 humidity (RH) were monitored using a thermohygrometer (HMP 45C, Campbell
165 Scientific, Logan, UT, USA). Net radiation (R_n) was quantified by a net radiometer (NR
166 Lite, Kipp and Zonen, Delft, Netherlands). **Soil heat flux (G) calculations, including the**

167 energy stored in the soil, were facilitated by one heat flux plate (HFP01SC, Hukseflux,
168 Delft, Netherlands) placed at 8 cm depth, complemented by three pairs of soil temperature
169 probes (TCAV, Campbell Scientific, Logan, UT, USA) situated at depths of 4 cm and
170 lateral distances of 3.20 m, 6.34 m, and 8.90 m from the tower.

171 The groundwater level (GWL) was monitored daily using a piezometer situated
172 within a well in the salt flats, approximately 2 kilometres south of the EC tower and on
173 the opposite side of the lake (37.1071° N, -4.7631° W; Fig S1). The location of the
174 piezometer coincides with the central and deepest part of the lake when there is water.
175 Negative GWL values indicate conditions when the lake is entirely lacking surface water.
176 Positive values measured by the piezometer were used to determine the lake depth.
177 Furthermore, data on daily precipitation (PPT), air temperature, and incident solar
178 radiation (spanning wavelengths from 350 to 1100 nm) were acquired from a
179 meteorological station located adjacent to Fuente de Piedra Lake, in Sierra Yeguas
180 (37.1383° N, -4.8358°; 467 m.a.s.l.). The tower setup and instruments were maintained
181 (mainly cleaning lenses of the open path sensors) every two weeks.

182

183 ***Greenhouse gas flux data processing, quality control and partitioning***

184 Half-hourly means (48 measurements per day), variances, and covariances of greenhouse
185 gas fluxes, adhering to the principles of Reynolds decomposition, were calculated using
186 the EddyPro® 7.0.7 software (Li-Cor), according to international standards and protocols
187 (Sabbatini et al., 2018). The data processing protocol encompassed the following steps:
188 (1) axis rotation for tilt correction using the double rotation method (Wilczak et al., 2001),
189 (2) turbulent fluctuations were calculated using block averaging method, (3) time lag was
190 compensated by covariance maximization with default, (4) Webb–Pearman–Leuning
191 (WPL) correction of air density fluctuation (Webb et al., 1980), (5) despiking and raw
192 data statistical screening (Vickers and Mahrt, 1997) and (6) spectral corrections of high-
193 and low-pass filtering effects. Regarding the latter, high-frequency loss due to path
194 averaging, signal attenuation and sensor separation was compensated according to
195 Moncrieff et al., (1997), whereas low-frequency loss due to finite time averaging length
196 and detrending was corrected according to Moncrieff et al. (2004). Quality check flags
197 were calculated for flux data according to the widely adopted methodology combining
198 two tests: steady state test and the developed turbulent conditions test. Over the study
199 period, we only selected high-quality fluxes (flag value =0) measured when the open-path
200 sensors were totally clean according to their respective Automatic Gain Control (AGC)

201 values (AGC value equal to or above 56 for Open path LI-7500A CO₂ /H₂O analyzer and
202 AGC value equal to or higher than 20 for LI-7700).

203 To quantify the sampling area of flux measurements, a footprint model was
204 estimated using the method by Kljun et al., (2004); **Fig 1**). Data periods when the wind
205 came from the terrestrial adjacent environment (251° to 59°) were rejected, representing
206 between 45% and 70% of the available daytime and night-time data respectively during
207 the dry season (GWL=0), and 30% of the available daytime and night-time data
208 respectively during the wet seasons (GWL>0). Overall, for the nearly 2 years of
209 measurements, 18% and 8% of the potential daytime data were of good quality for CO₂
210 and CH₄ fluxes respectively. While for night-time the available data were reduced to 10
211 and 5% respectively. In order to provide additional information regarding the turbulent
212 flux quality (Moncrieff et al 1997), we calculated the energy balance closure (ratio of the
213 sum of sensible and latent turbulent fluxes, H + LE, to the net radiation minus soil heat
214 flux, $R_n - G$) using all the available data during the drought period. The obtained value.
215 was 76% ($R^2 = 0.64$; $n = 3117$) and is within the range of most the reported FLUXNET
216 sites (Wilson et al 2022; Stoy et al., 2013)

217

218 *Predicting greenhouse gas fluxes as responses to meteorological drivers*

219 We examine the relationship of CO₂ and CH₄ fluxes in response to groundwater level,
220 serving as a proxy for long-term water storage, with air temperature as the main factor
221 regulating respiration in the system, and incident solar radiation modulating the
222 photosynthetic rate. Since these variables were measured every 24- hours, we processed
223 half-hourly CO₂ and CH₄ fluxes collected to construct 24-hour integrated values. It is
224 important to note that gaps in long-term data records are inevitable when using eddy
225 covariance, primarily due to instrument failure and insufficient turbulence (Falge et al.,
226 2001; Baldocchi et al., 2003; Aubinet et al., 2012). Additionally, data coverage is often
227 reduced when wind originates from undesirable sectors, though this does not necessarily
228 compromise measurement quality (Goloub et al., 2023). Despite these limitations, most
229 studies derive their primary results from annual or seasonal CO₂ and CH₄ balances using
230 various gap-filling procedures. In contrast, we exercise greater caution with our limited
231 data coverage, being very restrictive in quantifying daily fluxes. We selected dates with
232 over 50% of the anticipated data points, particularly those with more than 25 valid
233 measurements well-distributed throughout the day, to calculate integrated daily flux.
234 Before integrating daily flux values, we filled gaps in the half-hourly CO₂ and CH₄ flux

235 data using linear interpolation for missing values. This selection criterion aimed to
236 accurately represent the daily pattern in flux measurement distribution. Then, a
237 trapezoidal integration of the values measured every 30 minutes was performed to
238 calculate the daily flux.

239 To analyze the relationship between integrated daily fluxes and their potential
240 environmental predictors, we employed a linear regression combined with a forward
241 model selection technique (Aho et al 2014). This method involved sequentially fitting a
242 series of regression models, each incorporating different combinations of predictors and
243 their interactions. The process began with simple models, each containing only one
244 primary predictor, and gradually increased in complexity to include all possible
245 interactions among predictors. We then used the Akaike Information Criterion (AIC) to
246 evaluate and identify the most effective model from the set. The model with the lowest
247 AIC was selected as the best fit, indicating it provides the most useful balance between
248 model complexity and explanatory power. After selecting the model, we examined the
249 influence of the predictors by analyzing the slope β coefficients at a significance level of
250 $\alpha = 0.05$, using a 95% confidence interval to determine if these coefficients were
251 significantly different from zero. Additionally, while ground water level (GWL) was
252 measured daily, our model selection process also aimed to identify which daily
253 measurements of air temperature and incident solar radiation (mean, minimum, or
254 maximum) were the best predictors. This method ensured that the chosen model is robust
255 and relevant to the ecological scales being studied.

256 Finally, the chosen candidate model for predicting the fluxes in the system was
257 fitted using available records for the studied drivers, covering the period from 2001 to the
258 present at Fuente de Piedra Lake. This approach aimed to retrospectively model the fluxes
259 in the system. Detailed instructions on how to run these analyses are in the R script
260 available in DRYAD (see details in the *data accessibility statement* section).

261

262 3. Results

263 *Time series of greenhouse gas emissions and meteorological drivers*

264 At Fuente de Piedra Lake, we observed significant seasonal variations in meteorological
265 conditions, as illustrated in **Fig 2A**. Air temperature (T_a) and incident solar radiation
266 exhibited consistent trends throughout the study period, with mean daily values of 17 ± 7
267 °C for T_a and 18 ± 8 MJ m⁻² d⁻¹ for incident solar radiation. In contrast, these two

268 environmental variables generally followed asynchronous patterns with groundwater
269 level (GWL) and precipitation events, except for a brief peak in precipitation and an
270 increase in GWL between August and September 2021 (Fig. 2A and B). Particularly
271 during the summer months (July, August, September), the highest daily air temperature
272 values coincided with GWLs beneath the surface and a lack of precipitation. Also, during
273 dry conditions, a salt crust several centimeters thick developed on the sediment (see
274 Figure 3B). For instance, the minimum T_a recorded was 2 °C in January 2023
275 corresponding with a period of frequent precipitation and GWL above the surface.
276 Conversely, the maximum T_a of 34 °C occurred in August 2021, during a period when
277 the GWL was 24 cm below the surface.

278 After the study period, we were able to collect 4,128 measurements for CO₂ fluxes
279 and 2,425 measurements for CH₄ fluxes, which were relatively well-distributed over the
280 study period. We observed a strong correspondence between water storage in Fuente de
281 Piedra Lake and its capacity to assimilate atmospheric CO₂. The CO₂ flux patterns can be
282 categorized into two distinct lake states: a flooded lake (groundwater level >0 cm,
283 indicated from purple to blue colour in **Fig 2C and D**) and a dry lake (groundwater level
284 <0 cm, shown from orange to yellow colour). During flooding conditions, the lake acted
285 as a CO₂ sink, with fluxes ranging from 0 to -30 $\mu\text{mol m}^{-2} \text{s}^{-1}$. The CO₂ assimilation
286 capacity increases with groundwater level and incident solar radiation, particularly from
287 January to June. Notably, the flooded conditions in the two years of the study showed
288 marked differences in groundwater level. In 2022, we recorded the highest CO₂ uptake of
289 30 $\mu\text{mol m}^{-2} \text{s}^{-1}$ and an averaged value of -3.11 $\mu\text{mol m}^{-2} \text{s}^{-1}$ during May, when the
290 groundwater level was at its peak, 40 cm above the surface. This period was also
291 characterized by high variability in CO₂ flux, occasionally showing peaks of CO₂
292 outgassing approaching 20 $\mu\text{mol m}^{-2} \text{s}^{-1}$. The peak CO₂ uptake in 2023 was approximately
293 half of what was observed in 2022. Although this peak occurred in March rather than
294 May, it followed a similar trend to the ground water level (GWL), which was also about
295 half of the peak level observed in 2022 (~20 cm above the surface) resulting in averaged
296 CO₂ uptake values of -3.66 $\mu\text{mol m}^{-2} \text{s}^{-1}$. In contrast, under dry conditions, Fuente de
297 Piedra Lake ceases CO₂ uptake, occasionally transitioning to minor CO₂ emissions.
298 Notice that during extreme rainfall pulses within dry conditions, when Fuente de Piedra
299 Lake remained relatively dry with the groundwater level below the surface, we observed
300 notable net CO₂ emissions. For example, a heavy rainfall event in September 2021 (36
301 mm day⁻¹) resulted in CO₂ emissions reaching up to 10 $\mu\text{mol m}^{-2} \text{s}^{-1}$, with a high elevation

302 of the groundwater level above the surface (from -20 to near 20 cm). Also, in October of
303 both 2021 and 2022, subsequent rainfall events (12 mm day⁻¹ and 22 mm day⁻¹,
304 respectively) corresponded with CO₂ emissions of 7 μmol m⁻² s⁻¹ and 5.5 μmol m⁻² s⁻¹,
305 respectively. In these cases, emissions occurred under negative GWL conditions.

306 In the case of CH₄, the flux was relatively stable throughout the whole study
307 period, generally acting as a sink, with values fluctuating between -0.2 and 0.1 μmol m⁻²
308 s⁻¹ and an average of -0.05 μmol m⁻² s⁻¹ for the study period (Fig 2D). Furthermore, the
309 measured CH₄ fluxes did not seem to align clearly with the meteorological variables
310 examined (Fig S1).

311

312 *Fluxes of CO₂ and CH₄ at a daily scale*

313 When examining the daily scale during wet conditions, it becomes evident that CO₂
314 assimilation predominantly takes place during daylight hours, specifically between 9 a.m.
315 and 2 p.m. (local time) (Fig. 3). It should be noted that the few emission values observed
316 within this time frame correspond to the emission occurrences described earlier for the
317 dry season, which promptly followed rainfall events. In the case of dry condition, it is
318 noteworthy that a salt crust forms over the lake, leading to a near cessation of CO₂ fluxes.
319 In the case of CH₄, there is also a discernible increase in assimilation fluxes between 9
320 a.m. and 2 p.m. This observed pattern is consistent in both wet and dry conditions.

321

322 *Model predictions of 24-hour integrated flux values in the study system*

323 No evident relationship between CH₄ flux and the environmental predictors studied was
324 found during the study period. Additionally, measurements obtained from the EC tower
325 resulted in a substantial number of gaps in the CH₄ time series, making it impossible to
326 establish a predictive model for these fluxes. On the contrary, we were able to adjust a
327 robust regression model for CO₂ integrated daily flux. A total of 26 daily integrated CO₂
328 flux values were obtained for the sampling period, analyzing those dates when more than
329 25 valid measurements were available. After AIC model selection routine, the candidate
330 predictive model for daily integrated CO₂ flux was determined to include groundwater
331 level, maximum daily air temperature, and mean incident solar radiation. Additionally,
332 the model incorporated interactions between groundwater level and maximum daily air
333 temperature, as well as between groundwater level and incident solar radiation (Summary
334 Table of the model is available in the Supplementary Material). Indeed, fitted statistical
335 model has a relatively high explanatory capability (Adjusted R²=0.73).

336 The model confirmed a positive effect of groundwater level on enhancing CO₂
337 assimilation in the system (Fig 4A; $\beta_{GWL} = -0.115$, 95% CI = -0.214 to -0.016; note that
338 assimilation corresponds with negative values of the CO₂ flux). While the isolated impact
339 of air temperature increase on CO₂ assimilation could not be determined ($\beta_{Ta} = +0.07$,
340 95%CI = -0.053 to +0.192), the model identified an antagonistic interaction between air
341 temperature and groundwater level ($\beta_{GWL \times Ta} = +0.010$, 95%CI = +0.005 to +0.015). As
342 air temperature increases, the positive effect of GWL on CO₂ assimilation diminishes (Fig
343 4B). Conversely, mean daily incident solar radiation was found to promote CO₂
344 assimilation ($\beta_{Rad} = -0.12$, 95%CI = -0.21 to -0.03), with a pronounced synergy between
345 mean daily incident solar radiation and the presence of water ($\beta_{GWL \times Rad} = 95\%CI = -$
346 0.0116 to -0.003), notably enhancing the capacity for CO₂ assimilation (Fig 4C).

347 Using time series data for groundwater level, daily maximum air temperature, and
348 mean daily incident solar radiation at Fuente de Piedra Lake, we generated retrospective
349 predictions of CO₂ assimilation capacity in the system dating back to 2001 (Fig 4D). The
350 model predictions closely aligned with the observed values for the study period when
351 using the time series data for the predictors, supporting the robust predictive ability of our
352 model (Supplementary Material; Fig S2). Our estimates indicate a pronounced fluctuation
353 in CO₂ assimilation capacity according to hydrological variations. In years with higher
354 groundwater level and prolonged water storage the model predicted an exceptionally high
355 capacity for atmospheric CO₂ assimilation of the lake, with annual values surpassing 0.7
356 Kg C m⁻² year⁻¹ (e.g., in 2011, 2012, 2014, 2020). In contrast, during years marked by
357 extended droughts, a substantial reduction in CO₂ assimilation capacity was modeled,
358 with predicted reductions exceeding 80% compared to wetter years (Fig. 4D). These
359 drought periods, resulted in a reduction of the assimilation capacity to less than a third of
360 the levels recorded in wet years (e.g., from 2006 to 2010).

361

362 4. Discussion

363 In agreement with previous research on permanent saline lakes of the Tibetan plateau (Li
364 et al. 2022), we demonstrate that a model Mediterranean shallow saline lake serves as a
365 substantial carbon sink, absorbing atmospheric CO₂ when flooded. In particularly wet
366 years, expected uptake values can exceed -1.2 kg C m⁻² year⁻¹. Sporadic instances were
367 also observed where the system acted as a CO₂ emitter, resulting from rewetting events
368 that followed rainfall during dry conditions. Conversely, CO₂ uptake ceases during dry

369 conditions, reducing the system's capacity in dry years to below $-0.2 \text{ kg C m}^{-2} \text{ year}^{-1}$.
370 Longitudinal time series analysis reveals that prolonged droughts indeed hinder the ability
371 of the system to assimilate atmospheric CO_2 due to the lack of water, but we also observed
372 that an increase in air temperature during wet conditions moderates the CO_2 net
373 assimilation capacity, a process likely related to the reduction of gas water solubility with
374 temperature. This underscores the pronounced impact of seasonal and interannual
375 variability, ultimately dictated by drought and rainfall patterns, on the ability of the
376 studied system to sequester atmospheric carbon. Moreover, this pattern also displayed
377 considerable variability at the daily scale, closely correlating with fluctuations in incident
378 solar radiation over daily cycles. In this regard, the CO_2 assimilation capacity of the
379 system peaked during those hours of maximum incident solar radiation. While
380 measurement of CO_2 (and CH_4) fluxes at multiple scales is challenging and requires
381 specialized equipment (i.e. eddy covariance sensors), our research proposes an alternative
382 proxy. By integrating data from environmental predictors at various scales we have been
383 able to reconstruct the behavior of CO_2 exchanges between Fuente de Piedra Lake and
384 the atmosphere. In essence, we estimate CO_2 flux through the continuous measuring of
385 accessible environmental variables, namely, the amount of water, air temperature, and
386 incident solar radiation.

387 In shallow, well-mixed, and oxygenated systems like Fuente de Piedra Lake, the
388 photosynthetic capacity of the phytoplankton community is closely linked to the water
389 column height (i.e. groundwater level; Batanero et al. 2017), promoting CO_2 assimilation
390 as the extent of the habitat for these communities expands (Wetzel, 2001). Related to the
391 aforementioned, a significant synergy exists between water storage in the ecosystem and
392 incident radiation, serving as a proxy for the photosynthetically active radiation upon
393 which photosynthesis depends. This interaction occurs on both a daily scale, associated
394 with variations in light intensity following day-night cycles, and an annual seasonal scale,
395 largely determined by changes in daylight hours throughout the year. Notably, during the
396 night, the net exchange of CO_2 between the water and the atmosphere in Fuente de Piedra
397 Lake is negligible. This could be attributed to the absence of photosynthesis during
398 nighttime. Additionally, the high salinity inherent to these environments constrains
399 methanogenesis, which is the least energy-efficient carbon mineralization process in the
400 redox sequence (reviewed in Soued et al., 2024). Considering the above, it appears to
401 offer a plausible explanation for why microbial respiration does not surpass inorganic
402 carbon assimilation through photosynthesis in systems like Fuente de Piedra Lake during

403 wet conditions, despite the high content of dissolved organic carbon ranging between
404 1.00 and 13.59 mmol C L⁻¹ (Batanero et al., 2017).

405 What is more, despite the limited CH₄ flux data, our results position Fuente de
406 Piedra Lake as a CH₄ sink. Rough estimates determined that Fuente de Piedra could take
407 up on average 1.83 mg C m⁻² day⁻¹ and 3.70 mg C m⁻² day⁻¹ during wet and the dry
408 conditions respectively (Supplementary Material; Fig S3). Such values are even higher
409 than those measured in typical well aerated soils as in forests or grasslands, with average
410 rates of 0.4-1.26 mg C m⁻² day⁻¹ (Murguia-Flores et al., 2021; Perez-Quezada et al., 2021).
411 Twice the value of uptake during dry conditions compared to wet ones appear to be
412 consistent with some proposed mechanisms promoting CH₄ reduction according to the
413 existing literature, since the increase of temperature together with gas diffusivity due to
414 loss of water, may increase methane oxydation in a similar way to terrestrial ecosystems
415 (Chen et al., 2010; Rafalska et al 2023). However, caution is needed when interpreting
416 our results, as the dynamics of methane fluxes could become very complex in an
417 intermittent system like Fuente de Piedra. On the one hand, just as methanogenic activity
418 is inhibited by salinity (Herbert et al., 2015), methanotrophic activity has also been
419 observed to be significantly reduced by salinity in terrestrial systems (Ho et al., 2018).
420 However, methane oxydation processes associated with aquatic prokaryotes may be more
421 resistant to salinity (Khmelenina et al., 2010; Deng et al. 2017), especially if the variation
422 is gradual (Osudar et al., 2017). Thus, further measurements and analysis are needed to
423 estimate the role of methane oxydation and the relevance of saline intermitent lakes as
424 CH₄ sinks in a climate change scenario.

425 Drought conditions are accompanied by an increase in air temperature, with the
426 high air temperatures recorded immediately before the system completely dries out. We
427 have found that this rise in air temperature leads to a reduction of the system's capacity
428 to assimilate CO₂, even during wet conditions. A direct consequence of climatic warming
429 is the reduction of gas solubility accentuated in saline wetlands (Batanero et al. 2022). In
430 addition, an increase in temperature can enhance microbial metabolic rates and therefore,
431 biomass-specific CO₂ production (Smith et al. 2019). Given that endorheic saline lakes
432 are fueled by significant amounts of organic matter (Li et al., 2017; Batanero et al., 2017;
433 Song et al., 2013), it is unsurprising that warming leads to a decrease in net primary
434 production in the system as a result of enhanced microbial respiration, and consequently,
435 a reduction in CO₂ assimilation capacity. In addition, carbon emissions in inland waters
436 could increase with warming, independently of organic carbon inputs, simply because the

437 apparent activation energy is predicted to be higher for respiration than photosynthesis
438 (Yvon-Durocher et al. 2010; Yvon-Durocher et al. 2012). Finally, it has been recognized
439 that photosynthesis is often the first process to be affected by environmental stressors,
440 with photosynthetic capacity diminishing prior to other cellular functions (Feller, 2016;
441 Cardona et al., 2018). Specifically, carbon assimilation through the Calvin–Benson cycle
442 exhibits particular vulnerability to both drought and elevated temperatures, occurring
443 even when photosynthetic electron transport continues to operate effectively (Sharkey,
444 2005). On the whole, we show the profound synergy between global warming and
445 intensifying drought severity and frequency, disrupting the CO₂ assimilation capacity of
446 Mediterranean saline lakes and leading to negative feedback loops.

447 While the desiccation of saline lakes is not novel, with researchers highlighting
448 the concerning increase in dry periods within many of these ecosystems over recent
449 decades (Williams 1993; Gross 2017; Wurtsbaugh et al. 2017; Wang et al. 2018), our
450 study underscores the significant implications this trend has for the ecosystem services
451 they support. Our retrospective predictions show that in wet years, the system could
452 exhibit a high CO₂ assimilation rate. For instance, between 2010 and 2015, we estimated
453 that Fuente de Piedra Lake had an average assimilation rate of 0.83 (SD = ±0.27) kg C m⁻²
454 year⁻¹, within the same range as the net assimilation observed in evergreen or deciduous
455 forest systems worldwide (Pastorello et al., 2020) and marine salt marshes (Mayen et al.
456 2024). Considering the 13.6 km² area of Fuente de Piedra and assuming a constant flux
457 across the lake surface when flooded, we could estimate around 11 tons of carbon
458 sequestered during a wet and fully flooded year. Although this upscaling exercise is crude,
459 it highlights that Mediterranean shallow saline lakes could be a substantial carbon sink
460 and underline the potential relevance of keep them with water during their conservation
461 policies. Therefore, further studies across different Mediterranean shallow saline lakes
462 are necessary to refine these estimates and enhance our understanding of their role in the
463 global scale carbon budget.

464

465 **5. Conclusion**

466 Our result challenges the generalised belief that inland waters primarily act as sources
467 of greenhouse gases (Raymond et al. 2013). Conversely, the system undergoes significant
468 reductions in its annual atmospheric CO₂ sequestration capacity during dry conditions.
469 For instance, under severe drought conditions as observed in Fuente de Piedra from 2005

470 to 2009, the annual CO₂ sequestration is estimated to have fallen to less than a quarter of
471 what was observed in more humid conditions. Climate change projections, including even
472 the most optimistic scenarios, forecast an increase in both the frequency and duration of
473 heatwaves and droughts in the coming years (Trenberth 2011, Perkins-Kirkpatrick 2020).
474 This implies that saline lake ecosystems in arid and semi-arid endorheic basins will
475 remain dry for longer periods, or may even vanish, resulting in the loss of a significant
476 carbon sequestration pathway. Importantly, the disappearance of saline lakes due to water
477 scarcity has been largely attributed to anthropogenic water overuse (i.e., agriculture)
478 rather than to macroclimatic phenomena (Wurtsbaugh et al. 2017). This seems to be the
479 case of Fuente de Piedra Lake, as the catchment area is dominated by agricultural land.
480 Thus, a proper water **system** management during drought conditions seems to be the most
481 plausible solution to preserve the ecosystem services provided by Mediterranean saline
482 lakes.

483

484 **Author contribution**

485 PS-O and IR conceived the study; all authors contributed to the installation and
486 maintenance of the eddy covariance tower; IA led the fieldwork and the processing of the
487 samples with the help of the rest of the authors; IP-M carried out the analyses and the
488 preparation of the results; IA, IP-M, and PS-O conducted the preparation of the first draft
489 of the work; all authors participated in the drafting of the final draft.

490

491 **Data accessibility statement**

492 The R script used to conduct the data analysis and the datasets are available at the Dryad
493 Digital Repository:

494 <https://datadryad.org/stash/share/qEpPRJopVR132UaszL3bnaxoZh07ADL0E5LpVL6xC>

495 SZA

496

497 **Acknowledgements**

498 We thank the logistic support and groundwater level data provided by the curator of the
499 Natural Reserve of Laguna de Fuente de Piedra África Lupión Sánchez. Author also
500 acknowledge the review provided by the anonymous reviewers.

501

502 **Financial support**

503 This work was partially support by the projects PID2020-117825GB-C21 and PID2020-
504 117825GB-C22 funded by MCIN/AEI/10.13039/501100011033, LifeWatch-2019-10-
505 UGR-01 and LifeWatch-2019-09-CSIC-13 funded by the MCIN through the FEDER
506 funds from the Spanish Pluriregional Operational Program 2014-2020 (POPE),
507 LifeWatch-ERIC action line and project BAGAMET (P20_00016) funded by the
508 Counseling of Economy, Innovation, Science and Employment from the Government of
509 Andalucía, including European Union ERDF funds. I.P.-M. developed his research as
510 part of the eWARM project, supported by the Marie Skłodowska-Curie postdoctoral
511 fellowship 2022 (project number 101110111).

512

513 **Competing interests**

514 The authors declare that they have no conflict of interest.

515

516 **References**

517 Aho, K., Derryberry, D., and Peterson, T: Model selection for ecologists: the worldviews
518 of AIC and BIC. *Ecology*, 95(3), 631-636, <https://doi.org/10.1890/13-1452.1> ,
519 2014.

520 Anderson, L. G., Falck, E., Jones, E. P., Jutterström, S., and Swift, J. H: Enhanced uptake
521 of atmospheric CO₂ during freezing of seawater: A field study in Storfjorden,
522 Svalbard. *J. Geophys. Res. Oceans*, 109(C6)
523 <https://doi.org/10.1029/2003JC002120>, 2024.

524 Anderson, N. J., and Stedmon, C. A: The effect of evapoconcentration on dissolved
525 organic carbon concentration and quality in lakes of SW Greenland. *Freshwater*
526 *Biology*, 52(2), 280-289, <https://doi.org/10.1111/j.1365-2427.2006.01688.x> ,
527 2007.

528 Aubinet, M., Vesala, T., and Papale, D. *Eddy covariance: A practical guide to*
529 *measurement and data analysis*. London, UK Springer, 2012.

530 Baldocchi, D. D. Assessing the eddy covariance technique for evaluating carbon dioxide
531 exchange rates of ecosystems: past, present and future. *Glob. Chan. Biol.* 9(4),
532 479-492, <https://doi.org/10.1046/j.1365-2486.2003.00629.x> , 2003.

533 Batanero, G. L., León-Palmero, E., Li, L., Green, A. J., Rendón-Martos, M., Suttle, C.
534 A., and Reche, I. Flamingos and drought as drivers of nutrients and microbial

535 dynamics in a saline lake. *Scientific Reports*, 7(1), 12173,
536 <https://doi.org/10.1038/s41598-017-12462-9> , 2017.

537 Batanero, G. L., Green, A. J., Amat, J. A., Vittecoq, M., Suttle, C. A., and Reche, I.
538 Patterns of microbial abundance and heterotrophic activity along nitrogen and
539 salinity gradients in coastal wetlands. *Aquatic Sciences*, 84, 22,
540 <https://doi.org/10.1007/s00027-022-00855-6>, 2022.

541 Cardona, T., Shao, S., and Nixon, P. J: Enhancing photosynthesis in plants: the light
542 reactions. *Essays in biochemistry*, 62(1), 85-94,
543 <https://doi.org/10.1042/EBC20170015> , 2018.

544 Chen, W., Wolf, B., Zheng, X., Yao, Z., Butterbach-bahl, K. L. A. U. S., Brueggemann,
545 N., ... and Han, X: Annual methane uptake by temperate semiarid steppes as
546 regulated by stocking rates, aboveground plant biomass and topsoil air
547 permeability. *Glob. Change Biol.*, 17(9), 2803-2816.
548 <https://doi.org/10.1111/j.1365-2486.2011.02444.x> , 2011.

549 Comín, F. A., Julia, R., Comin, M. P., and Plana, F: Hydrogeochemistry of Lake
550 Gallocanta (Aragón, NE Spain). In *Saline Lakes: Proceedings of the Fourth*
551 *International Symposium on Athalassic (inland) Saline Lakes*, held at Banyoles,
552 Spain, May 1988 (pp 51-66). Springer Netherlands, 1990

553 Deng, Y., Liu, Y., Dumont, M., and Conrad, R. Salinity affects the composition of the
554 aerobic methanotroph community in alkaline lake sediments from the Tibetan
555 Plateau. *Microb. Ecol.*, 73, 101-110, <https://doi.org/10.1007/s00248-016-0879-5> ,
556 2017.

557 Duarte, C. M., Prairie, Y. T., Montes, C., Cole, J. J., Striegl, R., Melack, J., and Downing,
558 J. A: CO₂ emissions from saline lakes: A global estimate of a surprisingly large
559 flux. *J. Geophys. Res. G: Biogeosciences*, 113(G4),
560 <https://doi.org/10.1029/2007JG000637> , 2008.

561 Eugster, H. P., and Hardie, L. A. (1978). *Saline lakes*. In *Lakes: chemistry, geology,*
562 *physics* (pp. 237-293). New York, NY: Springer New York.

563 Falge, E., Baldocchi, D., Olson, R., Anthoni, P., Aubinet, M., Bernhofer, C., ... & Wofsy,
564 S. Gap filling strategies for long term energy flux data sets. *Agric. For. Meteorol.*
565 107(1), 71-77, [https://doi.org/10.1016/S0168-1923\(00\)00235-5](https://doi.org/10.1016/S0168-1923(00)00235-5) , 2001.

566 Feller, U: Drought stress and carbon assimilation in a warming climate: Reversible and
567 irreversible impacts. *J. Plant Physiol.*, 203, 84-94,
568 <https://doi.org/10.1016/j.jplph.2016.04.002> , 2016.

- 569 García, C. M., García-Ruiz, R., Rendón, M., Niell, F. X., and Lucena, J: Hydrological
570 cycle and interannual variability of the aquatic community in a temporary saline
571 lake (Fuente de Piedra, Southern Spain). *Hydrobiologia*, 345, 131-141,
572 <https://doi.org/10.1023/A:1002983723725> , 1997.
- 573 García, C. M., and Niell, F. X: Burrowing beetles of the genus *Bledius* (Staphylinidae) as
574 agents of bioturbation in the emergent areas and shores of an athalassic inland lake
575 (Fuente de Piedra, southern of Spain). *Hydrobiologia*, 215, 163-173,
576 <https://doi.org/10.1007/BF00014719> , 1991.
- 577 García, C. M., and Niell, F. X: Seasonal change in a saline temporary lake (Fuente de
578 Piedra, southern Spain). *Hydrobiologia*, 267(1), 211-223,
579 <https://doi.org/10.1007/BF00018803> ,1993.
- 580 Golub, M., Koupaei-Abyazani, N., Vesala, T., Mammarella, I., Ojala, A., Bohrer, G., et
581 al. Diel, seasonal, and inter-annual variation in carbon dioxide effluxes from lakes
582 and reservoirs. *Environ. Res. Lett.* 18(3), 034046, [https://doi.org/10.1088/1748-](https://doi.org/10.1088/1748-9326/acb834)
583 [9326/acb834](https://doi.org/10.1088/1748-9326/acb834) , 2023.
- 584 Guerrero, M. C., and Wit, R. d: Microbial mats in the inland saline lakes of Spain.
585 *Limnetica*, 8, 197–204, 1992.
- 586 Hammer, U. T: Saline lake ecosystems of the world. Springer Science and Business
587 Media, 1986.
- 588 Hardie, L. A., Smoot, J. P., and Eugster, H. P: Saline lakes and their deposits: a
589 sedimentological approach. *Modern and ancient lake sediments*, 7-41, 1978.
- 590 Hassani, A., Azapagic, A., D'Odorico, P., Keshmiri, A., and Shokri, N: Desiccation crisis
591 of saline lakes: A new decision-support framework for building resilience to
592 climate change. *Sci. Total Environ.*, 703, 134718,
593 <https://doi.org/10.1016/j.scitotenv.2019.134718> , 2020.
- 594 Heiri, O., Lotter, A. F., and Lemcke, G.: Loss on ignition as a method for estimating
595 organic and carbonate content in sediments: reproducibility and comparability of
596 results. *J. Paleolimnol.*, 25, 101-110, <https://doi.org/10.1023/A:1008119611481> ,
597 2001.
- 598 Khmelenina, V. N., Shchukin, V. N., Reshetnikov, A. S., Mustakhimov, I. I., Suzina, N.
599 E., Eshinimaev, B. T., and Trotsenko, Y. A.: Structural and functional features of
600 methanotrophs from hypersaline and alkaline lakes. *Microbiology*, 79, 472-482,
601 <https://doi.org/10.1134/S0026261710040090>, 2010.

602 Kljun, N., Calanca, P., Rotach, M. W., and Schmid, H. P.: A simple parameterisation for
603 flux footprint predictions. *Bound-Lay Meteorol.*, 112(3), 503–523,
604 <https://doi.org/10.1023/B:BOUN.0000030653.71031.96> , 2004.

605 Ho, A., Mo, Y., Lee, H. J., Sauheitl, L., Jia, Z., and Horn, M. A. Effect of salt stress on
606 aerobic methane oxidation and associated methanotrophs; a microcosm study of a
607 natural community from a non-saline environment. *Soil Biol. Biochem.*, 125, 210-
608 214, <https://doi.org/10.1016/j.soilbio.2018.07.013> , 2018.

609 Li, Y., Zhang, C., Wang, N., Han, Q., Zhang, X., Liu, Y., Xu, L. and Ye, W: Substantial
610 inorganic carbon sink in closed drainage basins globally. *Nature Geosci.*, 10(7),
611 501-506, <https://doi.org/10.1038/ngeo2972> ,2017.

612 Li, X. Y., Shi, F. Z., Ma, Y. J., Zhao, S. J., and Wei, J. Q: Significant winter CO₂ uptake
613 by saline lakes on the Qinghai-Tibet Plateau. *Glob. Change Biol.*, 28(6), 2041–
614 2052, <https://doi.org/10.1111/gcb.16054> , 2022.

615 Liao, Y., Xiao, Q., Li, Y., Yang, C., Li, J., and Duan, H: Salinity is an important factor in
616 carbon emissions from an inland lake in arid region. *Sci. Total Environ.*, 906,
617 167721, <https://doi.org/10.1016/j.scitotenv.2023.167721> , 2024.

618 Martínez-García, A., Peralta-Maraver, I., Rodríguez-Velasco, E., Batanero, G.L., García-
619 Alguacil, M., Picazo, F., Calvo, J., Morales-Baquero, R., Rueda, F.J., Reche, R:
620 Particulate organic carbon sedimentation triggers lagged methane emissions in a
621 eutrophic reservoir. *Limnol. Oceanogr. Lett.*, <https://doi.org/10.1002/lol2.10379> ,
622 2024.

623 Messenger, M. L., Lehner, B., Grill, G., Nedeva, I., and Schmitt, O: Estimating the volume
624 and age of water stored in global lakes using a geo-statistical approach. *Nature*
625 *comm.*, 7(1), 13603, <https://doi.org/10.1038/ncomms13603>, 2016.

626 Moncrieff, J. B., Massheder, J. M., de Bruin, H., Elbers, J., Friborg, T., Heusinkveld, B.,
627 Kabat, P., Scott, S., Soegaard, H., and Verhoef, A.: A system to measure surface
628 fluxes of momentum, sensible heat, water vapour and carbon dioxide. *J. Hydrol.*,
629 188–189, 589–611, [https://doi.org/10.1016/S0022-1694\(96\)03194-0](https://doi.org/10.1016/S0022-1694(96)03194-0) ,1997.

630 Moncrieff, J., Clement, R., Finnigan, J., and Meyers, T: Averaging, Detrending, and
631 Filtering of Eddy Covariance Time Series. In *Handbook of Micrometeorology*
632 (pp. 7–31), 2004.

633 Murguia-Flores, F., Ganesan, A. L., Arndt, S., and Hornibrook, E. R.: Global uptake of
634 atmospheric methane by soil from 1900 to 2100. *Global Biogeochem. Cycles*,
635 35(7), e2020GB006774, <https://doi.org/10.1029/2020GB006774> , 2021.

636 Osudar, R., Klings, K. W., Wagner, D., and Bussmann, I.: Effect of salinity on microbial
637 methane oxidation in freshwater and marine environments. *Aquatic Microb. Ecol.*,
638 80(2), 181-192, <https://doi.org/10.3354/ame01845> , 2017.

639 Pastorello, G., Trotta, C., Canfora, E., Chu, H., Christianson, D., Cheah, Y. W., ... & Law,
640 B.: The FLUXNET2015 dataset and the ONEFlux processing pipeline for eddy
641 covariance data. *Sci. Data*, 7, 225, <https://doi.org/10.1038/s41597-020-0534-3>,
642 2020.

643 Perez-Quezada, J. F., Urrutia, P., Olivares-Rojas, J., Meijide, A., Sánchez-Cañete, E. P.,
644 and Gaxiola, A.: Long term effects of fire on the soil greenhouse gas balance of
645 an old-growth temperate rainforest. *Sci. Total Environ.*, 755, 142442,
646 <https://doi.org/10.1016/j.scitotenv.2020.142442> , 2021.

647 Perkins-Kirkpatrick, S. E., and Lewis, S. C.: Increasing trends in regional heatwaves.
648 *Nature comm.*, 11(1), 3357, <https://doi.org/10.1038/s41467-020-16970-7> , 2020.

649 Rafalska, A., Walkiewicz, A., Osborne, B., Klumpp, K., and Bieganowski, A.: Variation
650 in methane uptake by grassland soils in the context of climate change—A review
651 of effects and mechanisms. *Sci. Total Environ.*, 871, 162127,
652 <https://doi.org/10.1016/j.scitotenv.2023.162127> , 2023.

653 Raymond, P. A., Hartmann, J., Lauerwald, R., Sobek, S., McDonald, C., Hoover, M., ...
654 and Guth, P.: Global carbon dioxide emissions from inland waters. *Nature*,
655 503(7476), 355-359, <https://doi.org/10.1038/nature12760> , 2013.

656 Rodríguez- Rodríguez, M., Benavente, J. and Moral, F.: High density ground-water flow,
657 major-ion chemistry and field experiments in a closed basin: Fuente de Piedra
658 Playa Lake (Spain). *American J. Environ. Sciences*. 1, 164–171, 2006.

659 Rysgaard, S., Glud, R. N., Lennert, K., Cooper, M., Halden, N., Leakey, R. J. G., and
660 Barber, D.: Ikaite crystals in melting sea ice—implications for pCO₂ and pH levels
661 in Arctic surface waters. *The Cryosphere*, 6(4), 901–908,
662 <https://doi.org/10.5194/tc-6-901-2012> , 2012.

663 Rysgaard, S., Søgaard, D. H., Cooper, M., Pućko, M., Lennert, K., Papakyriakou, T. N.,
664 and Barber, D.: Ikaite crystal distribution in Arctic winter sea ice and implications
665 for CO₂ system dynamics. *The Cryosphere*, 7(2), 707–718,
666 <https://doi.org/10.5194/tc-7-707-2013> , 2013.

667 Saccò, M., White, N. E., Harrod, C., Salazar, G., Aguilar, P., Cubillos, C. F., ... and
668 Allentoft, M. E. Salt to conserve: A review on the ecology and preservation of

669 hypersaline ecosystems. *Biol. Rev.*, 96(6), 2828-2850,
670 <https://doi.org/10.1111/brv.12780> , 2021.

671 Sabbatini, S., Mammarella, I., Arriga, N., Fratini, G., Graf, A., Hörtnagl, L., Ibrom, A.,
672 Longdoz, B., Mauder, M., Merbold, L., Metzger, S., Montagnani, L., Pitacco, A.,
673 Rebmann, C., Sedlák, P., Šigut, L., Vitale, D., and Papale, D.: Eddy covariance
674 raw data processing for CO₂ and energy fluxes calculation at ICOS ecosystem
675 stations. *Int. Agrophysics.*, 32(4), 495–515, [https://doi.org/10.1515/intag-2017-](https://doi.org/10.1515/intag-2017-0043)
676 [0043](https://doi.org/10.1515/intag-2017-0043) , 2018.

677 Sharkey, T. D.: Effects of moderate heat stress on photosynthesis: importance of
678 thylakoid reactions, rubisco deactivation, reactive oxygen species, and
679 thermotolerance provided by isoprene. *Plant Cell Environ.* 28(3), 269-277,
680 <https://doi.org/10.1111/j.1365-3040.2005.01324.x> , 2005.

681 Smith, T. P., Thomas, T. J., García-Carreras, B., Sal, S., Yvon-Durocher, G., Bell, T., and
682 Pawar, S.: Community-level respiration of prokaryotic microbes may rise with
683 global warming. *Nature comm.*, 10(1), 5124, [https://doi.org/10.1038/s41467-019-](https://doi.org/10.1038/s41467-019-13109-1)
684 [13109-1](https://doi.org/10.1038/s41467-019-13109-1) , 2019.

685 Song, K. S., Zang, S. Y., Zhao, Y., Li, L., Du, J., Zhang, N. N., ... and Liu, L.:
686 Spatiotemporal characterization of dissolved carbon for inland waters in semi-
687 humid/semi-arid region, China. *Hydrol. Earth Syst. Sci.*, 17(10), 4269-4281,
688 <https://doi.org/10.5194/hess-17-4269-2013> , 2013.

689 Soued, C., Bogard, M. J., Finlay, K., Bortolotti, L. E., Leavitt, P. R., Badiou, P., ... and
690 Kowal, P.: Salinity causes widespread restriction of methane emissions from small
691 inland waters. *Nature Comm.*, 15(1), 717, [https://doi.org/10.1038/s41467-024-](https://doi.org/10.1038/s41467-024-44715-3)
692 [44715-3](https://doi.org/10.1038/s41467-024-44715-3) , 2024.

693 Stoy, P. C., Mauder, M., Foken, T., Marcolla, B., Boegh, E., Ibrom, A., Arain, M. A.,
694 Arneeth, A., Aurela, M., Bernhofer, C., Cescatti, A., Dellwik, E., Duce, P.,
695 Gianelle, D., van Gorsel, E., Kiely, G., Knohl, A., Margolis, H., Mccaughey, H.,
696 ... Varlagin, A.: A data-driven analysis of energy balance closure across
697 FLUXNET research sites: The role of landscape scale heterogeneity. *Agric. For.*
698 *Meteorol.*, 171–172, 137–152, <https://doi.org/10.1016/j.agrformet.2012.11.004> ,
699 2013

700 Trenberth, K. E.: Changes in precipitation with climate change. *Clim. Res.* 47(1-2), 123-
701 138, <https://doi.org/10.3354/cr00953> , 2011.

702 Tweed, S., Grace, M., Leblanc, M., Cartwright, I., and Smithyman, D.: The individual
703 response of saline lakes to a severe drought. *Sci. Total Environ.*, 409(19), 3919-
704 3933, <https://doi.org/10.1016/j.scitotenv.2011.06.023> ,2011.

705 Vickers, D., and Mahrt, L.: Quality control and flux sampling problems for tower and
706 aircraft data. *J. Atmos. Ocean. Techno.*, 14(3), 512–526.,
707 [https://doi.org/10.1175/1520-0426\(1997\)014<0512:QCAFSP>2.0.CO;2](https://doi.org/10.1175/1520-0426(1997)014<0512:QCAFSP>2.0.CO;2) , 1997.

708 Wang, J., Song, C., Reager, J. T., Yao, F., Famiglietti, J. S., Sheng, Y., ..., and Wada, Y.:
709 Recent global decline in endorheic basin water storages. *Nature Geosci* 11, 926–
710 932, <https://doi.org/10.1038/s41561-018-0265-7> , 2018.

711 Webb, E. K., Pearman, G. I., and Leuning, R. Correction of flux measurements for density
712 effects due to heat and water vapour transfer. *Q. J. R. Meteorol. Soc.* 106 (447),
713 85–100, <https://doi.org/10.1002/qj.49710644707> ,1980

714 Wen, Z., Song, K., Shang, Y., Fang, C., Li, L., Lv, L., ... and Chen, L.: Carbon dioxide
715 emissions from lakes and reservoirs of China: a regional estimate based on the
716 calculated pCO₂. *Atmos. Environ.*, 170, 71-81,
717 <https://doi.org/10.1016/j.atmosenv.2017.09.032> , 2017.

718 Williams, W. D.: Environmental threats to salt lakes and the likely status of inland saline
719 ecosystems in 2025. *Environ. Conserv.*, 29(2), 154-167,
720 <https://doi.org/10.1017/S0376892902000103> , 2002.

721 Wilson, K., Goldstein, A., Falge, E., Aubinet, M., Baldocchi, D., Berbigier, P., ... &
722 Verma, S.: Energy balance closure at FLUXNET sites. *Agricultural and Forest*
723 *Meteorology*, 113(1–4), 223–243, [https://doi.org/10.1016/S0168-1923\(02\)00109-](https://doi.org/10.1016/S0168-1923(02)00109-0)
724 [0](https://doi.org/10.1016/S0168-1923(02)00109-0) , 2002.

725 Wu, Y., Wang, N., Zhao, L., Zhang, Z., Chen, L. I., Lu, Y., Lü, X., and Chang, J.:
726 Hydrochemical characteristics and recharge sources of Lake Nuertu in the
727 Badain Jaran Desert. *Sci. Bull.*, 59(9), 886–895 , [https://doi.org/10.1007/s11434-](https://doi.org/10.1007/s11434-013-0102-8)
728 [013-0102-8](https://doi.org/10.1007/s11434-013-0102-8) , 2014.

729 Wurtsbaugh, W. A., Miller, C., Null, S. E., DeRose, R. J., Wilcock, P., Hahnenberger,
730 M., ... and Moore, J.: Decline of the world's saline lakes. *Nat. Geosci.*, 10(11),
731 816-821, <https://doi.org/10.1038/ngeo3052> , 2017

732 Yan, L., and Zheng, M.: Influence of climate change on saline lakes of the Tibet Plateau,
733 1973–2010. *Geomorphology*, 246, 68-78,
734 <https://doi.org/10.1016/j.geomorph.2015.06.006> , 2015.

- 735 Yang, P., Wang, N. A., Zhao, L., Zhang, D., Zhao, H., Niu, Z., and Fan, G.: Variation
736 characteristics and influencing mechanism of CO₂ flux from lakes in the Badain
737 Jaran Desert: A case study of Yindeer Lake. *Ecol. Ind.*, 127, 107731,
738 <https://doi.org/10.1016/j.ecolind.2021.107731> , 2021.
- 739 Yvon-Durocher, G., Caffrey, J. M., Cescatti, A., Dossena, M., Giorgio, P. D., Gasol, J.
740 M., ... and Allen, A. P.: Reconciling the temperature dependence of respiration
741 across timescales and ecosystem types. *Nature*, 487(7408), 472-476,
742 <https://doi.org/10.1038/nature11205> , 2012.
- 743 Yvon-Durocher, G., Jones, J. I., Trimmer, M., Woodward, G. and Montoya, J. M:
744 Warming alters the metabolic balance of ecosystems. *Phil. Trans. R. Soc. B* 365,
745 2117–2126, <https://doi.org/10.1098/rstb.2010.0038> , 2010.

FIGURES

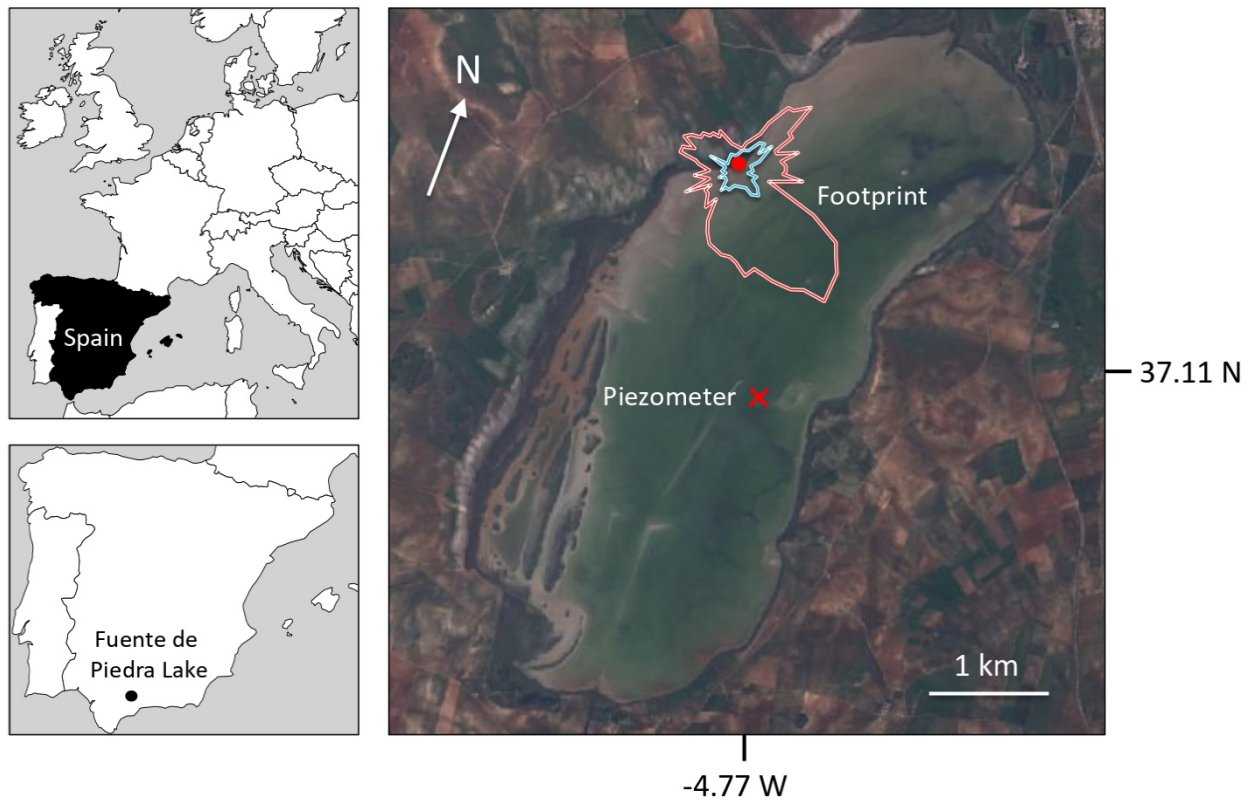


Fig 1. Location of the Fuente de Piedra Lake (province of Málaga, South of Spain). Dot inside polygon in right panel shows the location of the eddy covariance tower. The areas within the footprint contributing the 90% to measured fluxes are delimited inside polygons for daytime (blue) and nighttime (red). The cross indicates the location of the piezometer used for measuring groundwater level. Source image: Sentinel-2.

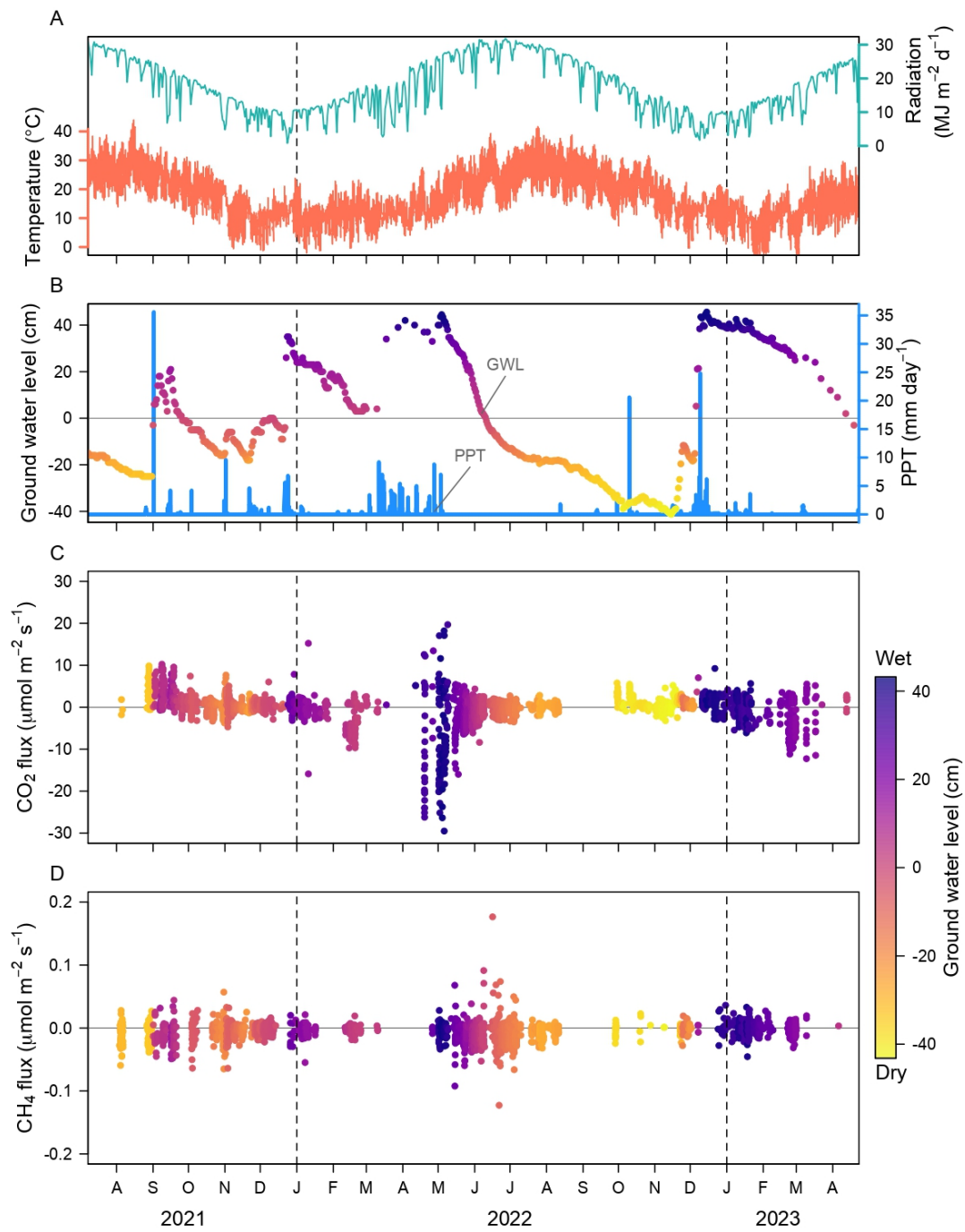


Fig 2. Time series of (A) air temperature and incident solar radiation, (B) groundwater level and precipitation (PPT), (C) CO₂ and (D) CH₄ flux, collected at Fuente de Piedra Lake during 2021, 2022, and 2023.

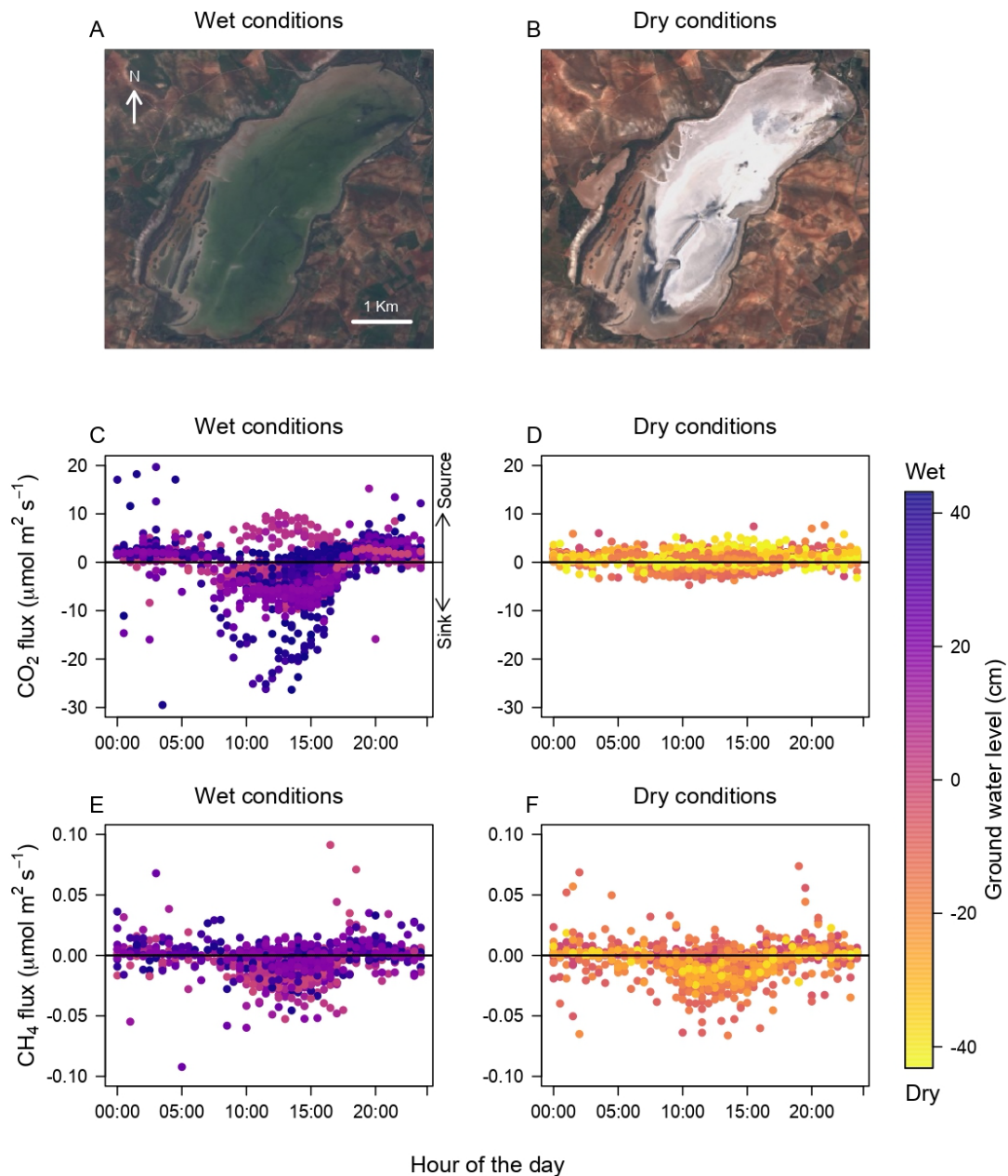


Fig 3. Aerial photos of Fuente de Piedra Lake during a period of maximum water availability (wet, **A**) and during a typical dry episode (**B**). Note that for some period during the dry episodes, a salt crust forms covering practically the entire extent of the lake. The figure shows the daily pattern of CO₂ and CH₄ fluxes during wet conditions (**C** and **E** respectively) and dry conditions (**D** and **F** respectively). Water availability is measured in terms of groundwater level. **Source image: Sentinel-2. Wet image was taken on 17-02-2021 and dry image was taken on 13-5-2021.**

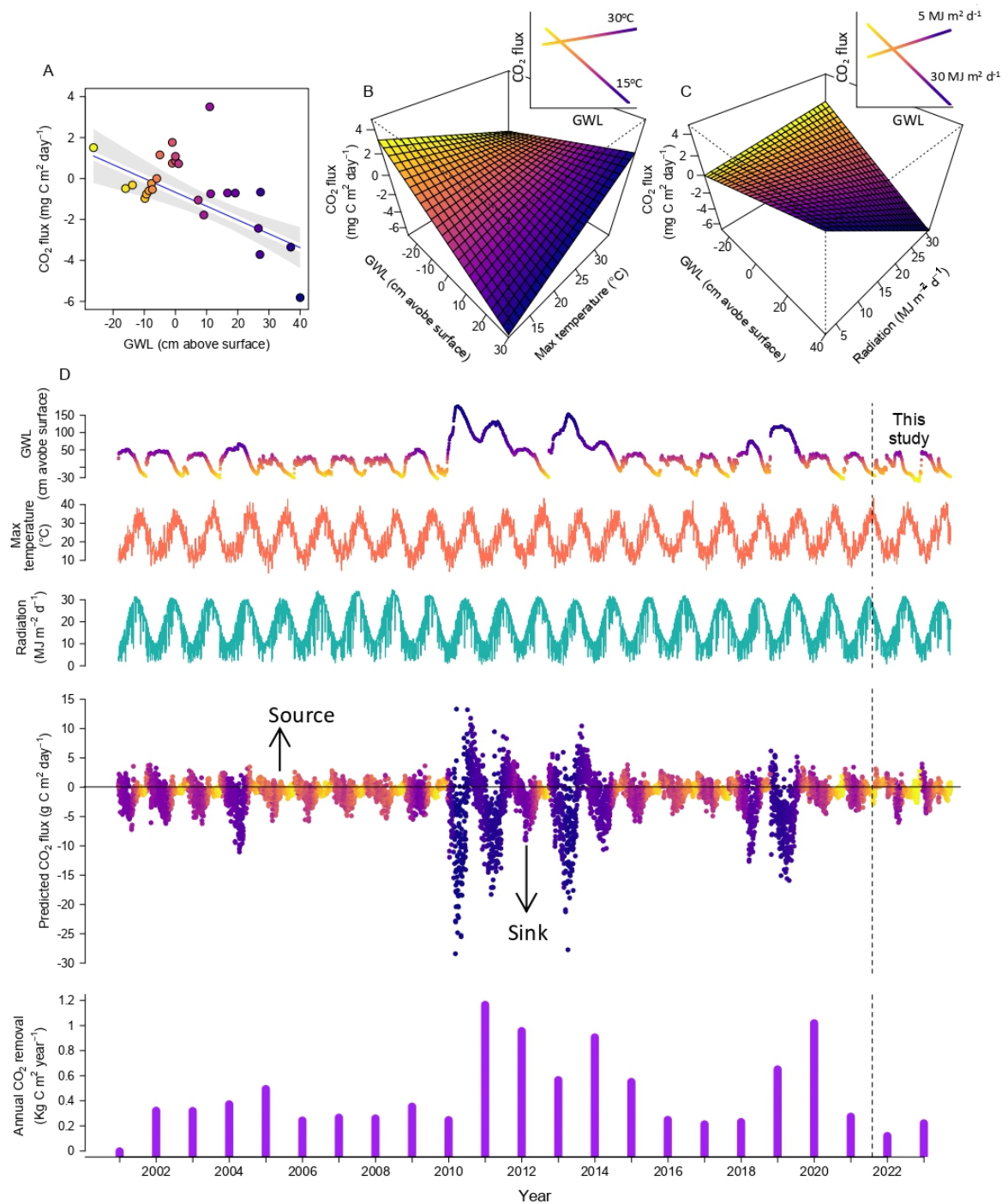


Fig 4. Prediction of CO₂ flux as a response to groundwater level with a slope of -0.115 (A), the interaction between groundwater level and daily maximum temperature (B), and the interaction between groundwater level and incident solar radiation (C). Model has an R² of 0.73. Using existing time series for the model predictors, it has been possible to reconstruct the estimated CO₂ fluxes, as well as the annual cumulative value of CO₂ removal since 2001 for Fuente de Piedra Lake (D).